Development 136, 615-625 (2009) doi:10.1242/dev.029355

Hand2 controls osteoblast differentiation in the branchial arch by inhibiting DNA binding of Runx2

Noriko Funato[1], Shelby L. Chapman[1], Marc D. McKee[2], Hiromasa Funato[3], Jesse A. Morris[4], John M. Shelton[4], James A. Richardson[1,5] and Hiromi Yanagisawa[1,*]

Members of the basic helix-loop-helix (bHLH) family of transcription factors regulate the specification and differentiation of numerous cell types during embryonic development. Hand1 and Hand2 are expressed by a subset of neural crest cells in the anterior branchial arches and are involved in craniofacial development. However, the precise mechanisms by which Hand proteins mediate biological actions and regulate downstream target genes in branchial arches is largely unknown. Here, we report that Hand2 negatively regulates intramembranous ossification of the mandible by directly inhibiting the transcription factor Runx2, a master regulator of osteoblast differentiation. Hand proteins physically interact with Runx2, suppressing its DNA binding and transcriptional activity. This interaction is mediated by the N-terminal domain of the Hand protein and requires neither dimerization with other bHLH proteins nor DNA binding. We observed partial colocalization of *Hand2* and *Runx2* in the mandibular primordium of the branchial arch, and downregulation of *Hand2* precedes Runx2-driven osteoblast differentiation. *Hand2* hypomorphic mutant mice display insufficient mineralization and ectopic bone formation in the mandible due to accelerated osteoblast differentiation, which is associated with the upregulation and ectopic expression of *Runx2* in the mandibular arch. Here, we show that Hand2 acts as a novel inhibitor of the Runx2-DNA interaction and thereby regulates osteoblast differentiation in branchial arch development.

KEY WORDS: Branchial arch, Intramembranous ossification, Neural crest, Craniofacial, Osteoblast, Mandible, Mouse

INTRODUCTION

The emergence of the jaw characterizes the evolution of vertebrates and is closely related to the development of neural crest cells (Sauka-Spengler et al., 2007; Shigetani et al., 2002). Primitive neural crest-like populations are present in cyclostomes, including hagfish (jawless, vertebraeless) and lamprey (jawless vertebrate), which are considered to be a sister group to the vertebrates (Ota et al., 2007). The identification of factors involved in the differentiation and regulation of cranial neural crest derivatives therefore provides insight into vertebrate evolution. Improper development of neural crest cells accounts for at least one-third of all birth defects in humans (Trainor, 2005). Syndromic mandibular dysmorphogenesis is common among craniofacial malformations, often accompanying clinical features of agnathia, micrognathia and macrognathia.

Hand1 and Hand2 are highly conserved basic helix-loop-helix (bHLH) proteins that are implicated in the development of the neural crest, heart, placenta and limb (Cross et al., 1995; Cserjesi et al., 1995; Riley et al., 1998; Srivastava et al., 1995). Gain-of-function studies have shown that Hand1 supports the proliferation of cardiac myocytes and prevents differentiation associated with cell-cycle exit (Risebro et al., 2006). Conversely, Hand1 induces differentiation of the trophoblast lineage by interacting with multiple bHLH proteins and Sox15 (Riley et al., 1998; Scott et al., 2000; Yamada et al., 2006). Neural crest-specific knockouts for *Hand2* demonstrated that Hand2 is necessary for the differentiation of catecholaminergic neurons in the sympathetic nervous system and of enteric neurons (D'Autreaux et al., 2007; Hendershot et al., 2008; Morikawa et al., 2007). The coordinated roles of Hand1 and Hand2 in heart and branchial arch development were demonstrated by generation of an allelic series of Hand mutant mice (Barbosa et al., 2007; McFadden et al., 2005; Yanagisawa et al., 2003). Furthermore, the regulation and mechanism of Hand functions have been investigated at a molecular level. Phosphorylation-dependent subnuclear localization of Hand1 is essential for cell fate determination of the trophoblast lineage (Firulli et al., 2003; Martindill et al., 2007). Gene dosage-dependent antagonistic interaction of *Hand2* and *Twist1*, as well as phosphorylation-regulated dimer choice between Hand2, Twist1 and E-proteins, have profound effects on limb and craniofacial development (Firulli et al., 2005; Firulli et al., 2007). Although Hand proteins act predictably according to bHLH models in vitro (Hollenberg et al., 1995; McFadden et al., 2002; Scott et al., 2000), biological functions of Hand proteins are largely dependent on cell type, and the precise molecular mechanisms of action of Hand proteins in the development of branchial arches are not fully understood. *Hand1* is expressed in the distal (ventral) zone of the first and second branchial arches, and the *Hand2* expression domain includes that of *Hand1* and extends laterally to occupy two-thirds of the branchial arches (Clouthier et al., 2000; Srivastava et al., 1997). An endothelin-1-dependent ventrolateral *Hand2* enhancer has been extensively characterized in vivo (Charité et al., 2001; Yanagisawa et al., 2003). Mice lacking this enhancer (termed $Hand2^{BA/BA}$) develop a spectrum of craniofacial defects, including hypoplastic mandible, cleft palate and abnormal middle ear ossicles, confirming the importance of *Hand2* expression driven by this enhancer in the development of subsets of cranial neural crest cells (Yanagisawa et al., 2003).

Craniofacial skeletons, which are derivatives of cranial neural crest cells, are formed preferentially by intramembranous ossification. Membranous bones are formed directly by osteoblast

[1]Department of Molecular Biology, [3]Department of Molecular Genetics, [4]Department of Internal Medicine and [5]Department of Pathology, University of Texas Southwestern Medical Center, Dallas, TX 75235, USA. [2]Department of Anatomy and Cell Biology, and Faculty of Dentistry, McGill University, Montreal, Quebec H3A 2B2, Canada.

*Author for correspondence (e-mail: hiromi.yanagisawa@utsouthwestern.edu)

Accepted 11 December 2008

differentiation of the condensed mesenchyme, whereas endochondral bones use cartilaginous templates that develop through endochondral ossification to form bones (Erlebacher et al., 1995). Runx2, one of three mammalian orthologs of the Runt-related transcription factor in *Drosophila*, is a crucial early determinant of the osteoblast lineage. Upregulation of *Runx2* is both necessary and sufficient to induce osteoblast differentiation by regulating expression of numerous osteoblast-specific genes, including *Runx2* itself (Ducy et al., 1997; Komori et al., 1997). Mutations in the *RUNX2* gene result in autosomal-dominant cleidocranial dysplasia in humans, which is characterized by hypoplasia/aplasia of clavicles, patent fontanelles, supernumerary teeth, short stature and other defects in skeletal patterning and growth (Mundlos et al., 1997; Otto et al., 1997). Here, we show that branchial arch-specific deletion of *Hand2* in mice results in a previously uncharacterized phenotype involving accelerated osteoblast differentiation. We provide molecular evidence of the function of Hand proteins, which involves direct interaction with, and inhibition of, Runx2 activity. These results reveal a novel role for Hand proteins as negative regulators of bone development, specifically in controlling the differentiation of osteoblasts derived from neural crest cells.

MATERIALS AND METHODS

Mutant animals

Hand2$^{BA/BA}$ and *Hand2-lacZ* mice have been described (Charité et al., 2001; Yanagisawa et al., 2003).

Cartilage and bone staining

Skeletal preparations were stained using Alcian Blue for cartilage and Alizarin Red for bone as described (McLeod, 1980).

Histology and in situ hybridizations

Paraffin-embedded sections were stained with Hematoxylin and Eosin (H&E) for routine histology or with von Kossa for detection of mineralization. In situ hybridization of sectioned tissues was performed as previously described (Shelton et al., 2000). Images were captured using Openlab 4.0.1 acquisition and analysis software (Improvision) and processed with Photoshop CS2 (Adobe).

β-galactosidase staining

β-galactosidase staining of transgenic embryos was performed as described (Yanagisawa et al., 1998).

Whole-mount in situ hybridization

Whole-mount in situ hybridization was performed as described (Barbosa et al., 2007). For whole-mount staining for alkaline phosphatase, embryos were stained with BM Purple (Roche) according to the manufacturer's instructions.

TUNEL and TRAP staining

TdT-mediated dUTP nick end labeling (TUNEL) staining was performed using the In Situ Cell Death Detection Kit (Roche) according to the manufacturer's protocol. Osteoclast activity was detected by staining for tartrate-resistant acid phosphatase (TRAP) using the Acid Phosphatase Leukocyte Kit (Sigma-Aldrich).

Immunostaining

Immunocytochemistry was performed as described (Funato et al., 2001). Phospho-histone H3 antibody (Upstate Biotechnology) was used according to the manufacturer's instructions to evaluate cell proliferation on paraffin-embedded sections.

Micro-computed tomography (Micro-CT)

An X-ray microtomograph (SkyScan1072, Kontich) was used to scan entire hemimandibles for 30 minutes at a rate of 1.9 seconds per scan (at 80 kV, 100 μA) using a rotational angle of 180° and a rotational step of 0.9°. For each sample, ~1000 X-ray slices, with increments of 15 μm covering the entire specimen, were reconstructed from the acquired scan. Three-dimensional reconstruction to visualize calcified tissue was performed based on triangular surface rendering using the manufacturer's software (3D-Creator). Measured parameters recorded for statistical analysis by the instrument and software included total mineralized tissue volume within each hemimandible (n=4).

Real-time quantitative PCR (qPCR)

Total RNA was isolated from mandibles (n=6-7 per genotype) using Trizol (Invitrogen) without pooling the samples. cDNA was synthesized using the Transcriptor First-Strand cDNA Synthesis Kit (Roche). qPCR was performed with an ABI Prism 7000 system using SYBR Green PCR Master Mix (Applied Biosystems) according to the manufacturer's instructions. Amplification of single products was confirmed by monitoring the dissociation curve. *Gapdh* mRNA level was used for normalization. Primer sequences are available upon request.

Cell culture and transfection assays

Expression vectors for Hand2, Hand1 and Runx2 deletions were generated by PCR. p6OSE2-luc and the expression vector for Twist1 were described previously (Ducy and Karsenty, 1995; Sosic et al., 2003). Reporter plasmid (100 or 150 ng) and indicated amounts of expression plasmids were transfected into COS cells using Fugene6 (Roche) with 50 ng of an RSV-β-galactosidase expression plasmid to monitor transfection efficiency. Cell extracts were prepared 48 hours after transfection and assayed for luciferase activity (Promega). To inhibit histone deacetylase (HDAC) activity, trichostatin A (TSA) (Sigma-Aldrich) at a final concentration of 100 nM, or an identical amount of ethanol (control), was added 24 hours before collecting cell lysates. For stable transfections, cells were selected using 400 μg/ml G418 and individual clones were harvested and amplified prior to analysis. Western blot analysis and immunostaining verified the presence of transgene in each clone analyzed, and more than four positive clones were combined for each stable cell line. For osteoblast differentiation assays, ROS 17/2.8 cells were grown to confluence and maintained in α-minimal essential medium (α-MEM) containing 10% FBS, with or without 10 mM β-glycerophosphate and 50 mg/ml ascorbic acid for the indicated number of days.

Co-immunoprecipitation (Co-IP) and western blotting

Cell lysates of COS cells transfected with the indicated expression constructs were harvested in lysis buffer [50 mM Tris-HCl (pH 7.4), 150 mM NaCl, 1 mM EDTA, 1% Triton X-100, 1× Roche complete protease inhibitor cocktail]. Lysates were incubated with specific-antibody-conjugated Protein G-Sepharose beads (Zymed) in lysis buffer with 0.1% BSA. Co-IP and western blotting were performed using rabbit anti-Myc (A14), mouse anti-Myc (9E10) (Santa Cruz Biotechnology) or mouse anti-Flag (M2; Sigma-Aldrich).

In vitro binding assays

Glutathione S-transferase (GST)-fusion proteins and maltose-binding protein (MBP)-tagged proteins were isolated from bacterial lysates using glutathione beads (Amersham) and amylose resin (NEB), respectively, according to manufacturers' directions. Glutathione beads conjugated with 2 μg of GST-fusion protein were incubated with 1 μg of MBP-tagged protein in NET buffer [50 mM Tris-HCl (pH 7.5), 100 mM NaCl, 5 mM EDTA, 0.5% NP40, 0.5% BSA]. The beads were then washed and eluted in 10 mM glutathione buffer. Elutes were subjected to SDS-PAGE, transferred to nitrocellulose membrane and immunoblotted using anti-Myc antibody.

Chromatin immunoprecipitation (ChIP) assays

ChIP assay was performed as described (Funato et al., 2003) with minor modifications. In brief, cells were formaldehyde cross-linked and lysed. Sheared chromatin was immunoprecipitated with anti-Runx2 antibody (M-70; Santa Cruz Biotechnology), and DNA was isolated and analyzed by PCR with osteocalcin gene primers. PCR primer sequences are available upon request.

Statistical analysis

The experimental data were analyzed by two-tailed Student's t-test and expressed as the mean ± s.e.m. A P-value less than 0.05 was considered significant.

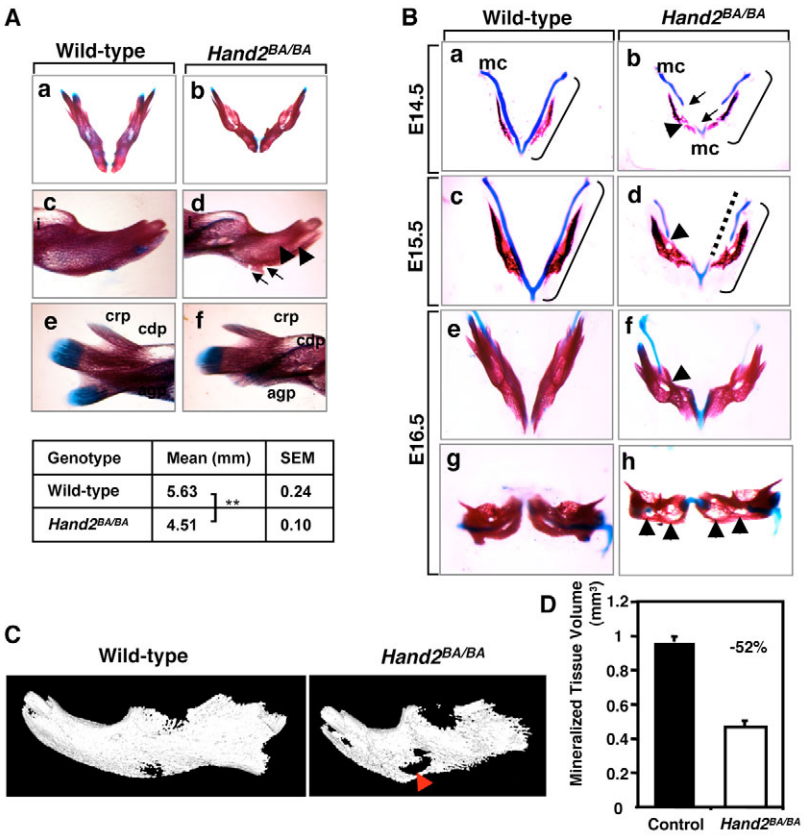

Fig. 1. Abnormal intramembranous ossification in *Hand2* mutant mice. (**A**) Bone staining of P1 mandibles from wild-type (a,c,e) and *Hand2*$^{BA/BA}$ (b,d,f) mice. (a,b) Ventral views of the mandible. The mandible in *Hand2*$^{BA/BA}$ is smaller and malformed with multiple sites lacking mineralized bone. Note the wider angle of the mutant mandible. (c,d) Lateral views of the mandibular body. Ectopic boney processes (arrows) and mineralized bone voids (arrowheads) are formed in mutants. (e,f) Lateral views of the mandibular processes. Angular process (agp) is hypoplastic in the mutants. i, lower incisor; crp, coronoid process; cdp, condylar process. Beneath is summarized the hemimandible length (mm) from wild-type and *Hand2*$^{BA/BA}$ mice (n=6 per genotype) at P1. $^{**}P<0.001$. (**B**) Skeletal preparations of mandibles at E14.5 (a,b), E15.5 (c,d) and E16.5 (e-h) from wild-type (a,c,e,g) and *Hand2*$^{BA/BA}$ (b,d,f,h) embryos. Interruption of Meckel's cartilage is evident in *Hand2*$^{BA/BA}$ at E14.5 (arrows in b). At E15.5 and E16.5 the mutant mandible is smaller and develops multiple mineralization voids (arrowheads). Brackets indicate mandibular length. (g,h) A lingual view of the mandible. mc, Meckel's cartilage. (**C**) Micro-CT of hemimandible from wild-type and *Hand2*$^{BA/BA}$ mice at P1. The mineralized mandible in *Hand2*$^{BA/BA}$ is smaller, deformed, and has a large void of mineralized tissue (arrowhead). (**D**) Mineralized tissue volume determined by micro-CT of a hemimandible from wild-type (control) and *Hand2*$^{BA/BA}$ mice (n=4 per genotype) at P1. The mandibles in *Hand2*$^{BA/BA}$ are less mineralized than in the control.

RESULTS

Accelerated osteoblast differentiation in the absence of *Hand2* expression

To investigate the role of Hand proteins in bone formation in the mandible, we used hypomorphic *Hand2*$^{BA/BA}$ mutants (Yanagisawa et al., 2003). Bone and cartilage staining with Alizarin Red and Alcian Blue, respectively, revealed hypoplastic mandibles with abnormal ossification in *Hand2*$^{BA/BA}$ mice at postnatal day (P) 1 (Fig. 1A). Membranous bones of the mandible appeared porous and ectopic bony processes were observed on the ventral surface of the mandible (Fig. 1Ad, arrowheads and arrows). The angular process was severely reduced in the mutants (Fig. 1Af, agp). The porotic bone phenotype was further confirmed by micro-CT, which indicated a 52% reduction of mineralized tissue volume in the *Hand2*$^{BA/BA}$ mice (Fig. 1C,D). The abnormal membranous bone phenotype provides strong support for the involvement of Hand proteins in the control of osteoblast differentiation.

To determine the onset of skeletal abnormalities in *Hand2*$^{BA/BA}$ embryos, we examined the mandible at several time points during intramembranous ossification (Fig. 1B). At embryonic day (E) 13.5, the mandible was indistinguishable between *Hand2*$^{BA/BA}$ and wild-type embryos (data not shown). By E14.5, *Hand2*$^{BA/BA}$ mandibular ossification proceeded despite an incomplete Meckel's cartilage template, resulting in a wider angle between the truncated mandible halves at E15.5 (arrows and interrupted line in Fig. 1Bb,d). In addition, multiple perforations were clearly evident within mature mandibular bones in *Hand2*$^{BA/BA}$ embryos by E15.5 (arrowheads in Fig. 1B), and this porotic phenotype became more prominent at E16.5 (Fig. 1Bh). By contrast, wild-type mandibular ossification occurred uniformly along the Meckel's cartilage and the mandible was smooth and compact (Fig. 1Bc,e). These data suggest that the osteoblast differentiation program is altered in *Hand2*$^{BA/BA}$ mutants.

During intramembranous ossification in the skull and ribs, the release of negative regulation is thought to be a prerequisite for *Runx2*-positive mesenchymal progenitors to initiate osteoblast differentiation (Bialek et al., 2004). The abnormal membranous bone in *Hand2*$^{BA/BA}$ mice suggested that the primary defect might involve control of osteoblast differentiation. To precisely define the molecular defects resulting from the absence of *Hand2* in the branchial arches, we assessed the activity and expression of known osteoblast differentiation markers: alkaline phosphatase (ALP; Alp1 – Mouse Genome Informatics), an early osteoblast differentiation marker expressed in preosteoblasts and post-proliferative osteoblasts; bone sialoprotein (*Bsp*; *Ibsp* – Mouse Genome Informatics), which is expressed predominantly in osteoblasts; and osteocalcin (*Bglap1/2* – Mouse Genome Informatics), an indicator of mature osteoblasts and osteocytes (Aubin et al., 1995). At E12.0, when the mandibular primordium is formed, ALP activity was barely detectable in wild-type embryos (Fig. 2Aa). By contrast, we detected a larger population of cells positive for ALP activity in *Hand2*$^{BA/BA}$ mutants (Fig. 2Ab). Although no significant upregulation of *Alp* or *Bsp* expression was detected by qPCR using whole-mandible RNA preparations (Fig. 2B), these results suggested that osteoblast differentiation had initiated in mutant embryos at E12.0. At E13.5, ALP activity was increased in the mandible of *Hand2*$^{BA/BA}$ as compared with wild-type embryos (Fig. 2Ca,d), specifically in the developing mandibular bone (Fig. 2Ac,d). *Bsp* and osteocalcin were also expanded in the mandible of *Hand2*$^{BA/BA}$ as compared with wild-type littermates (Fig. 2C), and the transcripts of all three markers were dramatically increased (Fig.

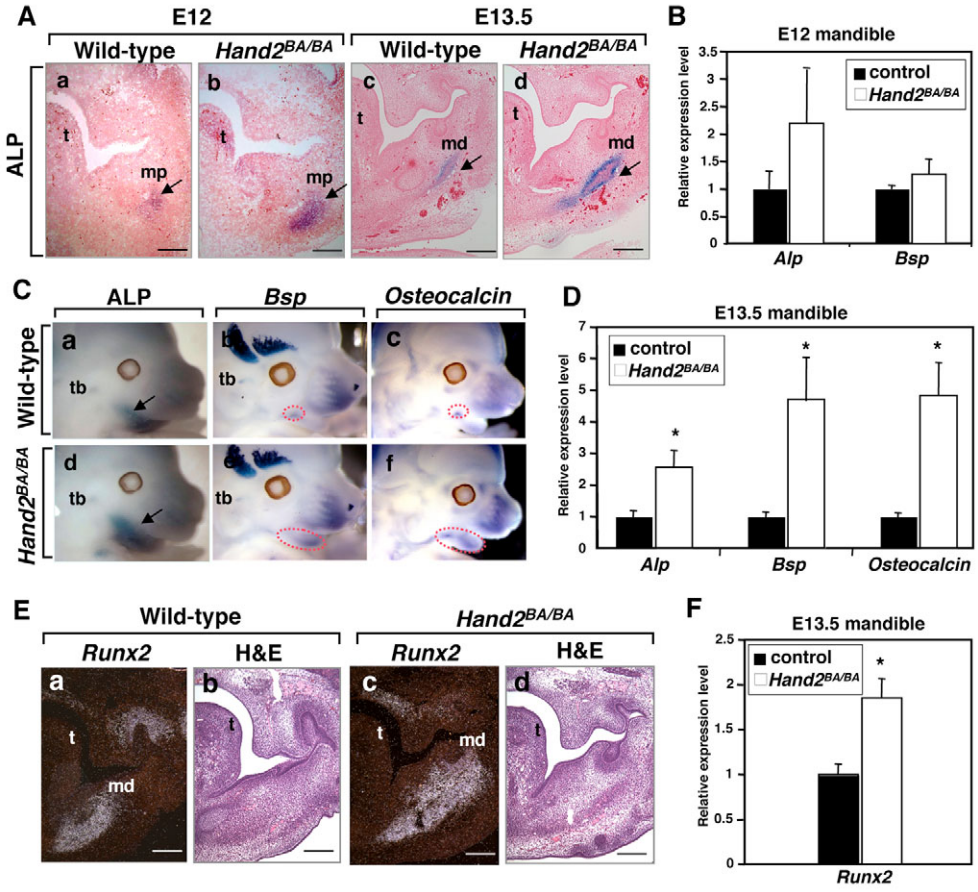

Fig. 2. Accelerated osteoblast differentiation in *Hand2*$^{BA/BA}$ embryos. (**A**) Evaluation of osteoblast differentiation in E12 (a,b) and E13.5 (c,d) mandibles from wild-type (a,c) and *Hand2*$^{BA/BA}$ (b,d) embryos by alkaline phosphatase (ALP) activity. ALP-positive mandibular primordium (mp, purple and arrows) and the mandibular bone (md and arrows) are expanded in *Hand2*$^{BA/BA}$ as compared with wild-type embryos. t, tongue. (**B**) qPCR analysis of *Alp* and *Bsp* transcripts in mandibles at E12. Differences observed between wild-type and *Hand2*$^{BA/BA}$ mandibles were not significant. (**C**) Detection of osteoblast differentiation markers in wild-type (a-c) and *Hand2*$^{BA/BA}$ (d-f) mandibles at E13.5. ALP activity (a,d), detected by whole-mount ALP staining, is upregulated in the mandible of *Hand2*$^{BA/BA}$ embryos as compared with the wild type (arrows), although activity in primordium of temporal bone (tb) is unchanged. Expression of *Bsp* (b,e) and osteocalcin (c,f), detected by whole-mount in situ hybridization, is expanded in *Hand2*$^{BA/BA}$. (**D**,**F**) Upregulation of *Alp*, *Bsp*, osteocalcin and *Runx2* expression in mandibles of *Hand2*$^{BA/BA}$ embryos at E13.5 as determined by qPCR. *P=0.031 for *Alp*, 0.043 for *Bsp*, 0.014 for osteocalcin and 0.0065 for *Runx2*. (**E**) The *Runx2* expression domain is expanded in E13.5 *Hand2*$^{BA/BA}$ mandible (c) as compared with the wild type (a) by section in situ hybridization. H&E staining of the adjacent sections is shown (b,d). Scale bars: 200 μm.

2D). Section in situ hybridization of E15.5 embryos also showed that the zone of *Bsp*- or osteocalcin-expressing cells extended further toward the midline in *Hand2*$^{BA/BA}$ than in wild-type mandible (see Fig. S1b,c,f,g in the supplementary material). Since TRAP staining showed no difference in osteoclast activity in the mutant mandible at E15.5 (data not shown), it is unlikely that a local increase in bone resorption was solely responsible for the porotic change. Furthermore, no difference was observed in the proliferation or apoptosis of mesenchymal cells in the mandibular arch between wild-type and *Hand2*$^{BA/BA}$ embryos at E11.5 and E13.5 (data not shown). Taken together, these findings indicate that *Hand2* insufficiency results in precocious and accelerated osteoblast differentiation in the mandible, which in turn leads to insufficient mineralization of the mandible.

Runx2 is a master regulator of bone differentiation and is capable of converting non-osteogenic cells to osteoblast-like cells in vivo (Ducy et al., 1997; Garg et al., 2005; Komori et al., 1997). Runx2 also binds its own promoter, establishing a positive autoregulatory loop (Ducy et al., 1999). Since ectopic bone formation was observed in *Hand2*$^{BA/BA}$ embryos (Fig. 1Ad), we speculated that the absence of Hand2 affected the expression of *Runx2*. Consistent with this hypothesis, the *Runx2* expression domain was expanded in the mandible of the mutant at E13.5 (Fig. 2Ea,c) and E15.5 (see Fig. S1d,h in the supplementary material), and the *Runx2* transcript level was markedly increased at E13.5 (Fig. 2F). These findings suggested that misregulation of *Runx2* expression/activity is an underlying molecular defect of abnormal intramembranous ossification in *Hand2*$^{BA/BA}$ mice.

Hand2 and *Runx2* expression during osteoblast differentiation

We performed in situ analysis to determine whether *Hand2* is expressed in a pattern compatible with a regulator of osteoblast differentiation. First, we analyzed *Hand1*, *Hand2* and *Runx2* expression in developing wild-type mandibles at E12.5 using whole-mount in situ hybridization. All three genes are expressed in the

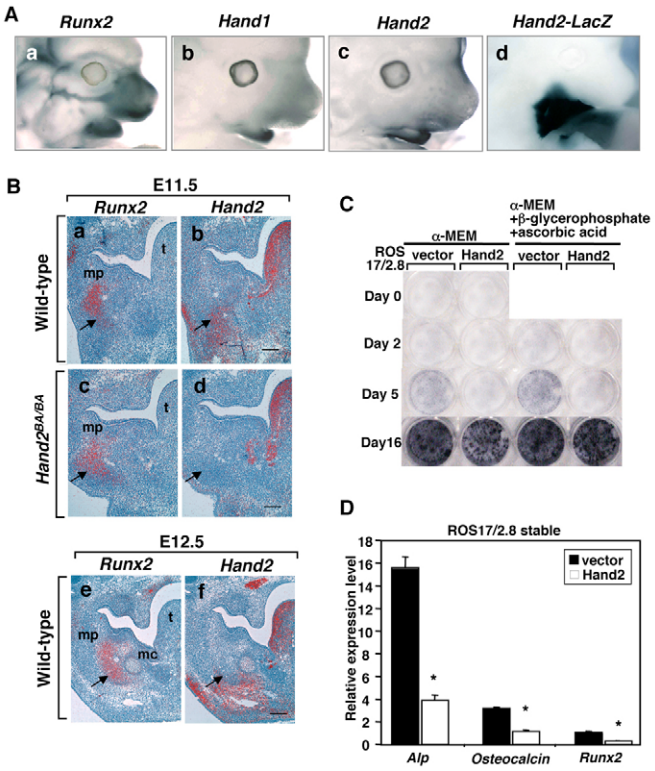

Fig. 3. Hand2 inhibits osteoblast differentiation. (**A**) Whole-mount in situ hybridization analysis of wild-type mouse embryos for *Runx2* (a), *Hand1* (b) and *Hand2* (c), and β-galactosidase staining of *Hand2-lacZ* (d) at E12.5. *Runx2*, *Hand1* and *Hand2* are colocalized in the mandibular arch. (**B**) Section in situ hybridization analysis of *Runx2* (a,c,e) and *Hand2* (b,d,f) in the branchial arch at E11.5 (a-d) and E12.5 (e,f) from wild-type (a,b,e,f) and $Hand2^{BA/BA}$ (c,d) embryos. At E11.5, *Runx2* and *Hand2* are partially colocalized in the mandibular primordium (mp) along the medial aspect in the wild-type embryo (arrow in a,b), whereas *Hand2* is not expressed in *Runx2*-expressing cells in $Hand2^{BA/BA}$ embryos (c,d). At E12.5, the overlapping expression domain of *Runx2* and *Hand2* is decreased in this region of the mandible. mc, Meckel's cartilage. Scale bars: 100 μm. (**C**) ALP activity of ROS17/2.8 cells stably transfected with empty vector or Myc-tagged *Hand2* expression vector. Cells were grown to confluence (day 0) and cultured in the indicated medium for 2, 5 or 16 days, then examined for ALP activity. Note the strong inhibition of the initiation of osteoblast differentiation by Hand2. (**D**) qPCR analysis of ROS17/2.8 cells cultured for 5 days in α-MEM as indicated in C. Expression of *Alp*, osteocalcin and *Runx2* is significantly reduced in *Hand2*-overexpressing cells. **P*=0.0009 for *Alp* and osteocalcin, 0.013 for *Runx2*.

mandibular arch (Fig. 3A) and *lacZ* expression driven by the 11 kb *Hand2* promoter recapitulates endogenous expression (Fig. 3Ad) (Charité et al., 2001).

Since the lateral *Hand2* expression domain does not overlap with that of *Hand1* (Yanagisawa et al., 2003), and no skeletal abnormalities are observed in $Hand1^{loxP/loxP}$; *Wnt1-Cre* mice (Barbosa et al., 2007), we focused our attention on Hand2. We examined, by in situ hybridization, the localization of *Hand2* and *Runx2* in the mandibular component of the first branchial arch prior to initiation of mandibular ossification. At E11.5, *Runx2* was expressed in the mandibular primordium (Fig. 3Ba) and *Hand2* expression modestly overlapped with the medial aspect of the *Runx2* expression domain in wild-type embryos (Fig. 3Bb). In $Hand2^{BA/BA}$ embryos, the *Runx2* expression domain was slightly expanded (Fig. 3Bc; Fig. 2E) and *Hand2* was absent from the corresponding region of the mandibular arch, although *Hand2* expression in the tongue and surrounding connective tissue was maintained (Fig. 3Bd). At E12.5, *Hand2* expression was decreased, and only overlapped with *Runx2* in the most medial component of the mandibular primordium (Fig. 3Be,f). Although we could not detect broad overlap between *Hand2* and *Runx2* in the mandibular primordium, we could not formally exclude the possibility that *Hand2* expression was below the detection limit of in situ hybridization. Expression analysis using *Hand2-lacZ* embryos, which recapitulate endogenous *Hand2* expression (Ruest et al., 2003), showed that the mandibular bone and surrounding connective tissues were positive for *lacZ*, exhibiting considerable overlap with *Runx2* expression at E12.5 (compare Fig. 3Be with Fig. S2a in the supplementary material). At E14.5, when osteoblast differentiation and intramembranous ossification occurs, *lacZ* expression was not detected in the mandible (see Fig. S2b, arrow, in the supplementary material). These data demonstrate that *Hand2* is transiently expressed in the primordium of mandibular bone and that *Runx2* induces intramembranous ossification after the decline in *Hand2* expression.

Hand2 is sufficient to inhibit osteoblast differentiation in vitro

Next, we asked whether Hand2 directly affects osteoblast differentiation. We stably transfected rat osteosarcoma ROS 17/2.8 osteoblastic cells with Hand2 or empty expression vectors. ROS 17/2.8 cells express markers for osteoblast progenitors, such as type I collagen (Bialek et al., 2004), and markers for differentiated osteoblasts, such as osteocalcin (Ducy et al., 1997), both of which are Runx2 target genes, but do not express *Hand1* or *Hand2* (data not shown). Upon induction of osteoblast differentiation in α-MEM medium with or without β-glycerophosphate and ascorbic acid, control ROS 17/2.8 cells sufficiently differentiated by day 5 (Fig. 3C). By contrast, in *Hand2*-overexpressing cells, differentiation was delayed. This was accompanied by marked reduction of *Alp*, osteocalcin and *Runx2* transcripts (Fig. 3D). These experiments indicate that Hand2 inhibits the initiation of osteoblast differentiation in vitro.

Hand proteins are Runx2 inhibitors

$Hand2^{BA/BA}$ mice exhibit ectopic bone formation and accelerated osteoblast differentiation in the first branchial arch. This phenotype, coupled with our observation that *Hand2* is expressed in mandibular primordium, led us to speculate that the initiation and/or progression of osteoblast differentiation might require release from Hand-mediated repression of Runx2. To address this possibility, we tested the effect of Hand proteins on the transcriptional activity of Runx2 in COS cells. Hand1 and Hand2 inhibited Runx2-dependent activation of luciferase activity through tandem copies of the Runx2 binding site (p6OSE2-luc) in a dose-dependent manner (Fig. 4A). To examine homo- or heterodimerization of Hand1 and Hand2 as a possible mechanism for repression of Runx2 activity, we used Hand2 with a phenylalanine-to-proline mutation in the first helix (mutant F119P), which is unable to dimerize with ubiquitous bHLH E-protein E12 (Tcfe2a – Mouse Genome Informatics) (McFadden et al., 2002). Hand2 (F119P) was unable to dimerize with Hand1 or Hand2 (Fig. 4C); however, it still inhibited Runx2 transactivation with Hand1 or Hand2 (Fig. 4B). Furthermore, Hand2 (ΔHLH), which lacks the domain necessary for dimerization with other bHLH proteins, showed similar results (Fig. 4B), confirming that neither a functional HLH motif nor dimerization with other bHLH proteins was required for Hand2 inhibitory function.

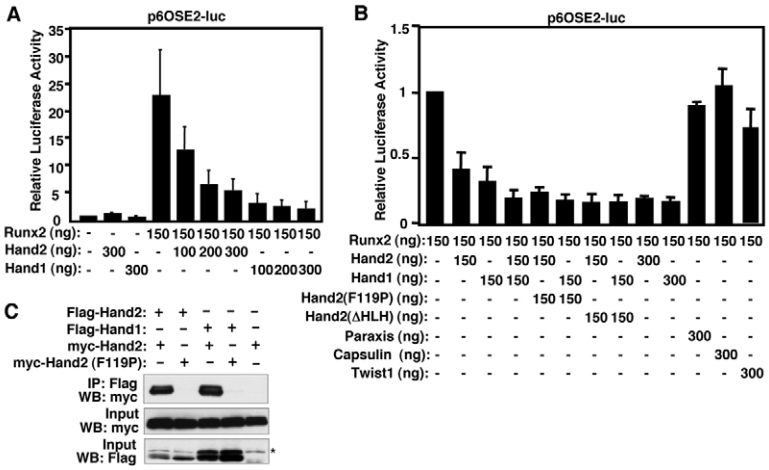

Fig. 4. Hand proteins inhibit Runx2 transactivation activity. (**A**) COS cells were transiently cotransfected with p6OSE2-luc reporter and the indicated amounts of expression vectors. Hand2 and Hand1 inhibited Runx2 transactivation in a dose-dependent manner. The data represent the mean ± s.e.m. (**B**) p6OSE2-luc reporter construct and Runx2 expression vector were transiently transfected alone or together with expression vectors encoding the indicated constructs. Hand2 and Hand1, Hand2 (F119P), or Hand2 (ΔHLH) inhibited Runx2-dependent transactivation. Paraxis and capsulin did not inhibit the Runx2 activity. Twist1 showed mild inhibition of Runx2 activity. Luciferase data are shown as percentage of Runx2 activation (normalized to 1.0). The data represent the mean ± s.e.m. (**C**) Co-IP assays. COS cells were transiently transfected with the indicated expression vectors. Flag-tagged Hand1 or Hand2 was immunoprecipitated (IP) from cell lysates with a monoclonal anti-Flag antibody, and co-immunoprecipitated Hand2 or Hand2 (F119P) was detected with anti-Myc antibody (top panel). Five percent of input samples were immunoblotted with an anti-Myc (middle panel) or anti-Flag (lower panel) antibody. The asterisk indicates a non-specific band.

To determine the specificity of Hand proteins in Runx2 inhibition, we tested the Hand-related bHLH proteins paraxis (Tcf15) (Burgess et al., 1995) and capsulin (Tcf21) (Funato et al., 2003) in this assay. Paraxis is 62% identical and 78% similar to Hand2 within the HLH domain (Burgess et al., 1995). Neither of these proteins was able to inhibit Runx2 transactivation function in this assay. Finally, we examined Twist1, which is abundantly expressed in developing branchial arches and was previously shown to dimerize with Hand2 upon phosphorylation and to function antagonistically to Hand2 (Firulli et al., 2005; Fuchtbauer, 1995). Although the expression of Twist1, Hand1 and Hand2 was comparable (data not shown), Twist1 itself only marginally inhibited Runx2-dependent transcription activity (Fig. 4B), and did not antagonize the Hand1 or Hand2 effect on Runx2 activity (data not shown). Taken together, these results indicate that Hand proteins possess a unique property that is not shared by the related bHLH protein paraxis, and that the inhibitory effects of Hand proteins are independent of dimerization with bHLH proteins.

Hand proteins interact directly with Runx2

To explore the mechanism by which Hand proteins mediate repression of Runx2 activity, we tested whether Hand proteins and Runx2 physically interact. As shown in Fig. 5A, Co-IP experiments demonstrated the association of Hand proteins with Runx2. In control experiments, Hand2 did not immunoprecipitate Smad2 (data not shown). In a cell-free system, GST-Runx2, but not GST, pulled down MBP-Hand2 and -Hand1, establishing that Hand proteins and Runx2 can interact directly (Fig. 5B). Hand1, Hand2 and Runx2 showed colocalization to the same intranuclear regions in cotransfected COS cells (Fig. 5C), consistent with the possible direct interaction of these proteins in vivo.

The transcriptional co-factors CREB-binding protein (CBP)/p300 (Crebbp – Mouse Genome Informatics) and four and a half LIM domains 2 (Fhl2), a member of the LIM-only subclass of the LIM protein superfamily, interact with Runx2 and increase its transcriptional activity (Gunther et al., 2005; Sierra et al., 2003). CBP/p300 physically interacts with Hand2 (Dai and Cserjesi, 2002) and Fhl2 is known to bind Hand1 and inhibit Hand1/E12 coactivation of a target gene reporter (Hill and Riley, 2004). However, neither CBP/p300 nor Fhl2 affected the ability of Hand2 to repress activation of Runx2-responsive reporters (Fig. 5D). Histone deacetylases (HDACs) are also known to directly interact with Runx2 and inhibit its transactivation activity (Vega et al., 2004); however, Hand-mediated repression was unaffected by the HDAC inhibitor TSA, suggesting that the repression was independent of HDAC catalytic activity (Fig. 5E).

The N-terminal domain of Hand2 inhibits Runx2 by binding to its Runt DNA-binding domain

We next searched for Runx2 domains that interact with Hand2. All Runx2 deletion mutants used in immunoprecipitation experiments contained an endogenous nuclear localization sequence (NLS) (Fig. 6A) and were expressed in nuclei (data not shown). Hand2 was immunoprecipitated by Runx2 and all deletion mutants except ΔRunt, which lacked the Runt DNA-binding domain (Fig. 6A,B). Conversely, the Runt domain alone was sufficient to bind Hand2 (Fig. 6A,B). These experiments establish that the Runt DNA-binding domain is necessary and sufficient for interaction with Hand2.

To identify the regions of Hand2 responsible for the inhibition of Runx2 function, we generated a series of Hand2 deletion mutants (Fig. 6C). Although some were also expressed in the cytoplasm, all deletion mutants were detectable and predominantly localized in the nucleus (Fig. 6E). Runx2 was immunoprecipitated by Hand2 deletion mutants Δ155-217, ΔHLH and Δbasic, but not Δ1-90 (Fig. 6D). Interestingly, although the C-terminal amino acids of Hand2 are highly conserved among all orthologs of Hand proteins, deletion of this region (155-217) still resulted in a marked reduction in the transcriptional activity of Runx2 (Fig. 6F). By contrast, Δ1-90 failed

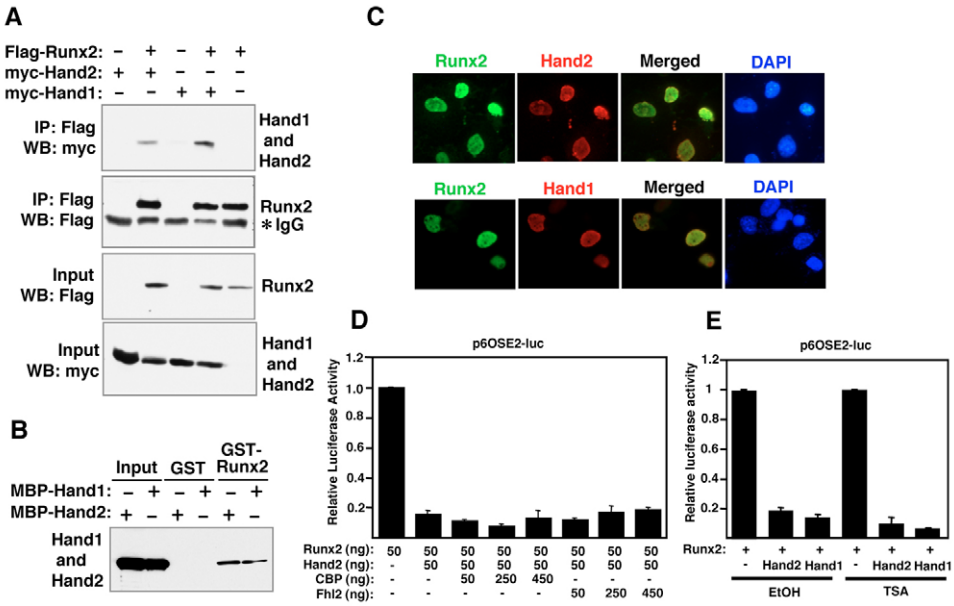

Fig. 5. Hand proteins interact directly with Runx2. (**A**) Co-IP assays. Flag-tagged Runx2 and Myc-tagged Hand1 or Hand2 were used as in Fig. 4C. (**B**) In vitro binding assays. Glutathione beads conjugated with GST-Runx2, or GST alone, were incubated with MBP-Myc-Hand1 or MBP-Myc-Hand2. Eluates from the beads were immunoblotted with anti-Myc antibody. GST-Runx2 and MBP-Hand2 or MBP-Hand1 showed direct interaction. (**C**) Subcellular localization of Hand proteins and Runx2. Myc-tagged Hand2 or Hand1, and Flag-tagged Runx2 were detected by immunostaining. Runx2, Hand1 and Hand2 colocalize in the nucleus. (**D**) p6OSE2-luc reporter was transiently transfected along with Runx2, Hand2 and increasing amounts of CBP or Fhl2 expression vector. The data represent the mean ± s.e.m. (**E**) Relative luciferase activity of Runx2 with Hand1 or Hand2 in the presence of TSA or ethanol (EtOH) control. The data represent the mean ± s.e.m.

to inhibit Runx2 transactivation function, and further analysis of the N-terminus showed that the Runx2 inhibitory domain of Hand2 was localized to amino acids 32-59 (Fig. 6C,F). Indeed, deletion of this region (Hand2 Δ32-59) completely abolished the binding and inhibition of Runx2 (Fig. 6D,F).

To determine whether the Runx2-inhibition domain is conserved between Hand1 and Hand2, we generated N-terminal deletion mutants of Hand1 (see Fig. S3A in the supplementary material). Hand1 (Δ32-59) was unable to interact with Runx2 (see Fig. S3B in the supplementary material). Although Hand1 (Δ32-59) and Hand1 (Δ1-87) mutants localized to the nucleus (see Fig. S3C in the supplementary material), they failed to inhibit Runx2-mediated transcriptional activity (see Fig. S3D in the supplementary material). We conclude that Hand protein binding to Runx2 is responsible for repression of Runx2 activity (Fig. 6C).

Finally, to determine whether direct DNA binding is required for Hand2 activity in our transactivation assay, we used a DNA-binding mutant of Hand2 (RRR109-111EDE) (McFadden et al., 2002) in which three conserved arginine residues in the basic region were mutated (Fig. 6C). As Fig. 6F shows, the RRR109-111EDE mutant was a potent repressor of Runx2, indicating that Hand2 does not require direct DNA binding to inhibit Runx2 transactivation function.

Detection of Hand2-Runx2 interaction by ChIP

The observation that Hand2 interacts with the Runx2 DNA-binding domain suggested that Hand2 might also inhibit the DNA-binding activity of Runx2. To address this, we examined the effect of Hand2 on Runx2 association with the osteocalcin promoter by ChIP of extracts from ROS 17/2.8 cells stably transfected with full-length Hand2, Hand2 (Δ1-90) or Hand2 (Δ32-59) expression vectors. As shown in Fig. 6Ga,b, the association of Runx2 with the osteocalcin promoter was readily detectable by ChIP assay in the presence of Hand2 (Δ1-90) or Hand2 (Δ32-59), and this interaction was abolished in the presence of wild-type Hand2. We conclude that the association of Hand2 with the Runt domain of Runx2 interferes with DNA binding by Runx2 and, consequently, inhibits activation of Runx2 target genes (Fig. 7A).

DISCUSSION

The results presented here demonstrate that Hand2 regulates osteoblast differentiation and intramembranous ossification in the mandible by negatively regulating the transcriptional activity and expression of *Runx2* in vivo. The interaction between the Runt DNA-binding domain of Runx2 and the N-terminal domain of Hand2 provides a molecular basis for the inhibitory effect of Hand2 on osteoblast differentiation. The following observations support this conclusion. (1) *Hand2* mutant mice display ectopic bone formation and insufficient mineralization of the mandible associated with accelerated osteoblast differentiation and upregulation of *Runx2*. (2) *Hand2* and *Runx2* expression domains overlap at the medial aspect of mandibular primordium, and intramembranous ossification occurs after the decline in *Hand2* expression. (3) Overexpression of Hand2 in vitro effectively inhibits the initiation of osteoblast differentiation. (4) Hand proteins physically associate with Runx2, thereby inhibiting the DNA binding and transcriptional activity of Runx2.

Regulation of osteoblast differentiation by Hand proteins

Our current findings, coupled with recently published work, suggest that Hand proteins have multiple roles in craniofacial development, as depicted in Fig. 7B. Hand proteins are involved in

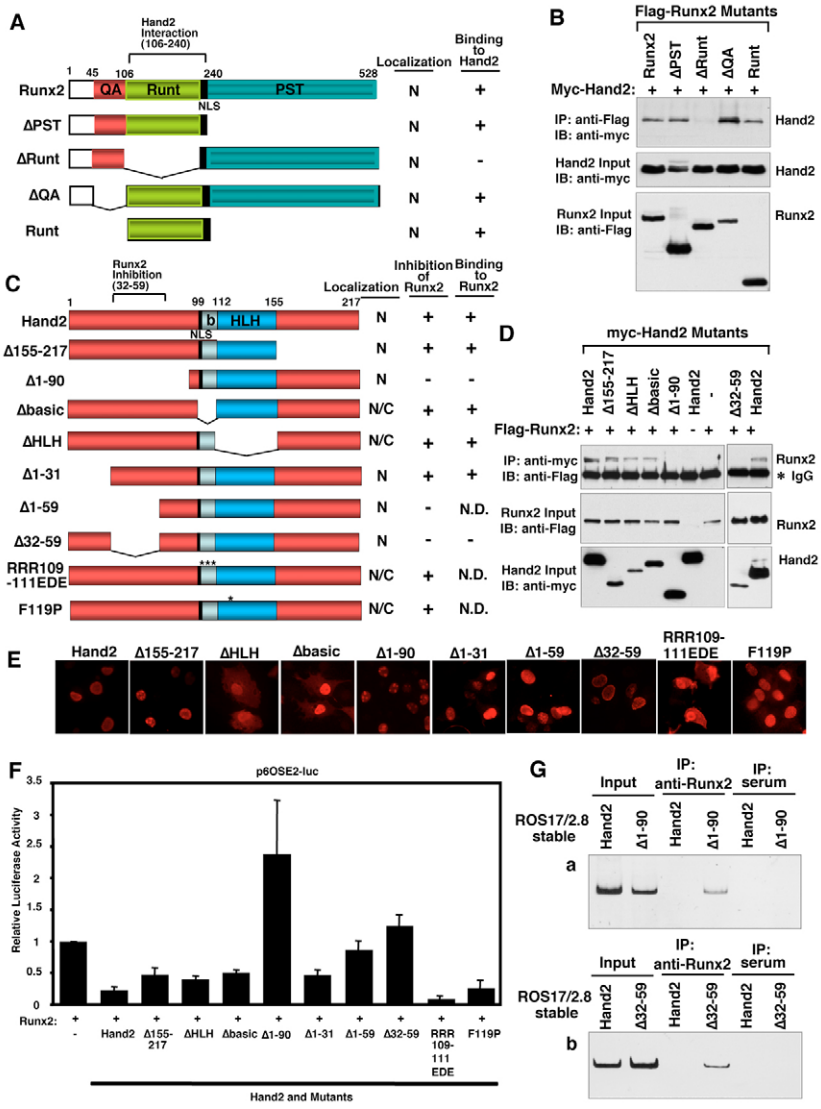

Fig. 6. Inhibition of Runx2 DNA-binding function by the N-terminal domain of Hand2. (**A**) Schematic of Runx2 functional domains and deletion mutants. All mutants contain an N-terminal Flag-epitope tag. Runt, Runt DNA-binding domain; QA, glutamine/alanine repeats; PST, proline/serine/threonine-rich region; NLS, nuclear localization signal; N, nucleus. (**B**) Mapping the Hand2-interaction domain of Runx2 by Co-IP assays. COS cells were transfected with expression plasmids encoding Flag-tagged Runx2 deletion mutants (as shown in A) and Myc-tagged Hand2. Flag-Runx2 was immunoprecipitated with an anti-Flag antibody, followed by western blot analysis to detect Myc-Hand2 binding. (**C**) Schematic of Hand2 functional domains and deletion mutants. All mutants contained an N-terminal Myc-epitope tag. b, basic DNA-binding domain; HLH, helix-loop-helix; NLS, nuclear localization signal; N, nucleus; C, cytoplasm, N.D., not determined. Asterisks indicate point mutations. (**D**) Mapping the Runx2-interaction domain of Hand2 by Co-IP assays. COS cells were transfected with expression vectors encoding Myc-tagged Hand2 deletion mutants (as shown in C) and Flag-tagged Runx2. Myc-Hand2 was immunoprecipitated with an anti-Myc antibody, followed by western blot analysis to detect Flag-Runx2 binding. (**E**) Subcellular localization of wild-type and mutant Hand2 proteins. Hand2 proteins expressed in COS cells were examined by immunocytochemistry. (**F**) Identification of the Runx2-inhibition domain of Hand2. p6OSE2-luc reporter was transiently transfected along with Runx2 expression vectors and the various Hand2 deletion mutants (as shown in C). Fold activity measured in the absence of Hand2 was normalized to 1.0. The data represent the mean ± s.e.m. (**G**) ChIP assays were performed using soluble chromatin prepared from ROS17/2.8 cells stably transfected with Hand2, Hand2 (Δ32-59) or Hand2 (Δ1-90) vector, as indicated. Chromatin was immunoprecipitated with non-immune rabbit IgG or Runx2 antibodies as indicated. Precipitated genomic DNA was analyzed by PCR using primers for the osteocalcin promoter, which contains a Runx2-binding OSE2 site. An input control, in which PCR amplification was performed prior to immunoprecipitation, is also shown. Hand2 specifically perturbs the association of Runx2 with its target sequence on the osteocalcin promoter, whereas Hand2 (Δ1-90) (a) or Hand2 (Δ32-59) (b) shows no effect.

the early development of postmigratory neural crest cells by maintaining and/or patterning subsets of neural crest cells. Failure to maintain the distal midline mesenchyme in *Hand1/2* compound mutant embryos (Barbosa et al., 2007), and the interrupted Meckel's cartilage and hypoplastic angular process in *Hand2*$^{BA/BA}$ mice, may be attributable to the loss of Hand functions in patterning or maintenance of neural crest cells at the early post-migratory stage.

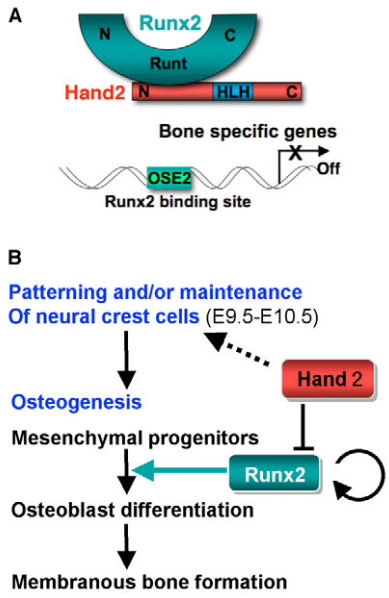

Fig. 7. Molecular mechanism of Runx2 regulation by Hand proteins. (**A**) Hand2 directly binds Runx2 and blocks its transcriptional activity. Hand2 binds the Runt DNA-binding domain of Runx2, thereby preventing access to its target sequence in the promoters of bone-specific genes. N, N-terminal; C, C-terminal; HLH, helix-loop-helix; OSE2, Runx2 binding site. (**B**) A model for regulation of osteoblast differentiation in the branchial arch by Hand2. Hand2 is required in early development of postmigratory neural crest cells and their derivatives, and subsequently during osteogenesis in the first branchial arch. Function of Runx2, which is necessary and sufficient for osteoblast differentiation and which controls the rate of bone formation by osteoblasts, is transiently inhibited by Hand2.

At early stages of mandible development, *Hand2* modulates osteoblast differentiation by inhibiting *Runx2* in the primordium of mandibular bone. *Runx2* expression was detected in the mandibular primordium at E11.5, yet expression of the early osteoblast marker ALP was not clearly detectable until E13.5, and intramembranous ossification of the mandibular bone did not occur before E14.5. This time-lag between *Runx2* expression and execution of osteoblast differentiation implies that multiple layers of regulation are required in bone formation, and that Hand proteins are one of the regulators involved in this process.

Marker gene expression analyses of $Hand2^{BA/BA}$ embryos indicate that the loss of Hand2 leads to upregulation of *Runx2* expression/activity, resulting in accelerated osteoblast differentiation, ectopic bone formation and compromised mineralization of the mandible. The precise mechanism of the compromised mineralization is not fully understood, although it might be attributable to a depletion of the reserves of osteoblast precursors as a result of accelerated differentiation. Consequently, a decrease, over time, in the number of bone mineralization-regulating osteoblasts and/or an increase in the non-functional osteoblasts could lead to reduced mineralized tissue volume. A similar concept was presented for the detrimental effect of premature differentiation on the tissue-regenerative function of myocytes owing to depletion of the reserves of progenitors (Brack et al., 2008). However, we cannot formally exclude the possibility that abnormal osteoblasts in $Hand2^{BA/BA}$ embryos affected the function of osteoclasts, which are linked to osteoblast differentiation (Engin et al., 2008). Taken together, these data suggest a model in which Hand2 controls proper temporal and spatial expression of osteoblast differentiation genes by regulating Runx2.

Mechanism of Runx2 repression by Hand proteins

The expression and activity of Runx2 must be regulated to prevent aberrant ossification or delayed bone development. Our current study establishes that Hand proteins tightly regulate Runx2 activity in the branchial arches. We propose two mutually compatible mechanisms for the regulation of Runx2 by Hand proteins. First, Runx2 is a primary target of Hand2 repression in vivo. The absence of Hand2 might accelerate the positive autoregulatory loop of Runx2. Second, Hand2 physically interacts with Runx2 and inhibits its ability to transactivate promoters of osteoblast-specific Runx2 target genes. This repression does not require recruitment of HDAC proteins or HDAC activity and no interaction was detected between Hand2 and Hdac5, a class II HDAC expressed in the developing craniofacial skeleton (data not shown). Rather, the inhibitory function is through direct interaction between Hand2 and Runx2, as we observed by ChIP assays. The repressive influence of Hand proteins must then be released in a timely manner for Runx2 to bind osteoblast-specific gene promoters and execute osteoblast differentiation in the branchial arch.

Interestingly, this type of repression that causes ‘sequestration’ of DNA-binding factors in the nucleus is similar to previously reported inhibitory functions of Hdac4 and Twist1 on Runx2 (Bialek et al., 2004; Vega et al., 2004). However, the biological impact of Hdac4 and Twist1 inhibition is distinct from that of Hand proteins in several aspects. Hdac4 expression is restricted to chondrocytes and *Hdac4*-null mice show acceleration of chondrocyte hypertrophy and, consequently, precocious endochondral mineralization (Vega et al., 2004). By contrast, the phenotype of Hand mutant mice reflects a defect in osteoblast differentiation and maturation in the branchial arch. The possibility exists that Hand2 affects chondrocyte maturation by regulating the antagonistic function of Runx2 on *Fgf18* at the perichondrium (Hinoi et al., 2006) and/or on Indian hedgehog, which is a target gene of Runx2 that is expressed in pre-hypertrophic chondrocytes (Yoshida et al., 2004), as *Hand2* is also expressed in these regions of the developing ulna (McFadden et al., 2002). Whereas both *Hdac4*-null mice and *Hand2* mutant mice show ectopic bone formation with upregulation of *Runx2* expression in vivo, Twist1 inhibits osteoblast differentiation in the skull and ribs without affecting *Runx2* expression and without the development of ectopic bones or insufficient mineralization (Bialek et al., 2004).

Hand2 function is independent of DNA binding and dimerization

The bHLH domain of Hand proteins has been considered to be essential for their function. However, our data show that the repressive function of Hand2 on Runx2 does not require the basic region, suggesting that the underlying mechanism is independent of E-box-mediated transcriptional regulation. In addition, Hand2 mutants lacking DNA-binding activity (RRR109-111EDE) or HLH protein-binding activity (F119P) are as potent as the wild-type protein in inhibiting Runx2-dependent transcriptional activation, indicating that Hand2 uses a mechanism independent of direct DNA binding or dimerization with other bHLH proteins. Antagonistic interaction between Hand2 and Twist1 has been implicated in Saethre-Chotzen syndrome (Firulli et al., 2005). However, Twist1 did not antagonize the effect of Hand1 or Hand2 on Runx2 transcriptional activity. Our results clearly show that Hand proteins

can use a mechanism that is different from the conventional functional model of bHLH proteins to exert their functions according to cell type and biological process.

Function of the N-terminal domain of Hand2

Molecular evidence establishes that the anti-osteogenic function of Hand proteins is mediated by an N-terminal domain that is distinct from its bHLH domains. We showed that Hand2 (Δ32-59) and Hand1 (Δ32-59) could not inhibit Runx2 transactivation function. *hand2* zebrafish mutant alleles were identified in a screen for mutations affecting heart, jaw and pectoral fin development, including a null allele completely deleting the *hand2* locus (han^{s6}) and a truncated allele lacking the N-terminal domain (han^{c99}) (Yelon et al., 2000). Interestingly, the han^{c99} mutant exhibited continuous upper jaw joints, and the deletion is equivalent to amino acids 1-53 of mouse *Hand2* (Miller et al., 2003). Although the N-terminal domain of Hand2 is conserved among jawed vertebrates, including stickleback, pufferfish and zebrafish, it is not conserved in fruit fly or sea squirt (our unpublished observations), suggesting that this N-terminal region might exert a crucial biological function required for jaw formation. One may speculate that gene elongation at the N-terminus of Hand might have occurred upon evolution of vertebrates from lower chordates. Sequence analysis of Hand genes in agnathans might provide a link between the N-terminal domains of Hand genes and the appearance of neural crest and/or jaw development.

We thank Rhonda Bassel-Duby, Gerard Karsenty, Ana Barbosa, Ning Liu, Masataka Nakamura and Masao Saitoh for reagents, and Eric Olson and Vidu Garg for critical reading of the manuscript. This work was supported by grants from the March of Dimes Birth Defects Foundation (H.Y.), the Cleft Palate Foundation (H.Y.) and the Canadian Institutes of Health Research (M.D.M.). N.F. was supported by the JSPS Postdoctoral Fellowships for Research Abroad 2005.

Supplementary material

Supplementary material for this article is available at http://dev.biologists.org/cgi/content/full/136/4/615/DC1

References

Aubin, J. E., Liu, F., Malaval, L. and Gupta, A. K. (1995). Osteoblast and chondroblast differentiation. *Bone* **17**, 77S-83S.

Barbosa, A. C., Funato, N., Chapman, S., McKee, M. D., Richardson, J. A., Olson, E. N. and Yanagisawa, H. (2007). Hand transcription factors cooperatively regulate development of the distal midline mesenchyme. *Dev. Biol.* **310**, 154-168.

Bialek, P., Kern, B., Yang, X., Schrock, M., Sosic, D., Hong, N., Wu, H., Yu, K., Ornitz, D. M., Olson, E. N. et al. (2004). A twist code determines the onset of osteoblast differentiation. *Dev. Cell* **6**, 423-435.

Brack, A. S., Conboy, I. M., Conboy, M. J., Shen, J. and Rando, T. A. (2008). A temporal switch from notch to Wnt signaling in muscle stem cells is necessary for normal adult myogenesis. *Cell Stem Cell* **2**, 50-59.

Burgess, R., Cserjesi, P., Ligon, K. L. and Olson, E. N. (1995). Paraxis: a basic helix-loop-helix protein expressed in paraxial mesoderm and developing somites. *Dev. Biol.* **168**, 296-306.

Charité, J., McFadden, D. G., Merlo, G., Levi, G., Clouthier, D. E., Yanagisawa, M., Richardson, J. A. and Olson, E. N. (2001). Role of Dlx6 in regulation of an endothelin-1-dependent, dHAND branchial arch enhancer. *Genes Dev.* **15**, 3039-3049.

Clouthier, D. E., Williams, S. C., Yanagisawa, H., Wieduwilt, M., Richardson, J. A. and Yanagisawa, M. (2000). Signaling pathways crucial for craniofacial development revealed by endothelin-A receptor-deficient mice. *Dev. Biol.* **217**, 10-24.

Cross, J. C., Flannery, M. L., Blanar, M. A., Steingrimsson, E., Jenkins, N. A., Copeland, N. G., Rutter, W. J. and Werb, Z. (1995). Hxt encodes a basic helix-loop-helix transcription factor that regulates trophoblast cell development. *Development* **121**, 2513-2523.

Cserjesi, P., Brown, D., Lyons, G. E. and Olson, E. N. (1995). Expression of the novel basic helix-loop-helix gene eHAND in neural crest derivatives and extraembryonic membranes during mouse development. *Dev. Biol.* **170**, 664-678.

D'Autreaux, F., Morikawa, Y., Cserjesi, P. and Gershon, M. D. (2007). Hand2 is necessary for terminal differentiation of enteric neurons from crest-derived precursors but not for their migration into the gut or for formation of glia. *Development* **134**, 2237-2249.

Dai, Y. S. and Cserjesi, P. (2002). The basic helix-loop-helix factor, HAND2, functions as a transcriptional activator by binding to E-boxes as a heterodimer. *J. Biol. Chem.* **277**, 12604-12612.

Ducy, P. and Karsenty, G. (1995). Two distinct osteoblast-specific cis-acting elements control expression of a mouse osteocalcin gene. *Mol. Cell. Biol.* **15**, 1858-1869.

Ducy, P., Zhang, R., Geoffroy, V., Ridall, A. L. and Karsenty, G. (1997). Osf2/Cbfa1: a transcriptional activator of osteoblast differentiation. *Cell* **89**, 747-754.

Ducy, P., Starbuck, M., Priemel, M., Shen, J., Pinero, G., Geoffroy, V., Amling, M. and Karsenty, G. (1999). A Cbfa1-dependent genetic pathway controls bone formation beyond embryonic development. *Genes Dev.* **13**, 1025-1036.

Engin, F., Yao, Z., Yang, T., Zhou, G., Bertin, T., Jiang, M. M., Chen, Y., Wang, L., Zheng, H., Sutton, R. E. et al. (2008). Dimorphic effects of Notch signaling in bone homeostasis. *Nat. Med.* **14**, 299-305.

Erlebacher, A., Filvaroff, E. H., Gitelman, S. E. and Derynck, R. (1995). Toward a molecular understanding of skeletal development. *Cell* **80**, 371-378.

Firulli, B. A., Howard, M. J., McDaid, J. R., McIlreavey, L., Dionne, K. M., Centonze, V. E., Cserjesi, P., Virshup, D. M. and Firulli, A. B. (2003). PKA, PKC, and the protein phosphatase 2A influence HAND factor function: a mechanism for tissue-specific transcriptional regulation. *Mol. Cell* **12**, 1225-1237.

Firulli, B. A., Krawchuk, D., Centonze, V. E., Vargesson, N., Virshup, D. M., Conway, S. J., Cserjesi, P., Laufer, E. and Firulli, A. B. (2005). Altered Twist1 and Hand2 dimerization is associated with Saethre-Chotzen syndrome and limb abnormalities. *Nat. Genet.* **37**, 373-381.

Firulli, B. A., Redick, B. A., Conway, S. J. and Firulli, A. B. (2007). Mutations within helix I of Twist1 result in distinct limb defects and variation of DNA binding affinities. *J. Biol. Chem.* **282**, 27536-27546.

Fuchtbauer, E. M. (1995). Expression of M-twist during postimplantation development of the mouse. *Dev. Dyn.* **204**, 316-322.

Funato, N., Ohtani, K., Ohyama, K., Kuroda, T. and Nakamura, M. (2001). Common regulation of growth arrest and differentiation of osteoblasts by helix-loop-helix factors. *Mol. Cell. Biol.* **21**, 7416-7428.

Funato, N., Ohyama, K., Kuroda, T. and Nakamura, M. (2003). Basic helix-loop-helix transcription factor epicardin/capsulin/Pod-1 suppresses differentiation by negative regulation of transcription. *J. Biol. Chem.* **278**, 7486-7493.

Garg, V., Muth, A. N., Ransom, J. F., Schluterman, M. K., Barnes, R., King, I. N., Grossfeld, P. D. and Srivastava, D. (2005). Mutations in NOTCH1 cause aortic valve disease. *Nature* **437**, 270-274.

Gunther, T., Poli, C., Muller, J. M., Catala-Lehnen, P., Schinke, T., Yin, N., Vomstein, S., Amling, M. and Schule, R. (2005). Fhl2 deficiency results in osteopenia due to decreased activity of osteoblasts. *EMBO J.* **24**, 3049-3056.

Hendershot, T. J., Liu, H., Clouthier, D. E., Shepherd, I. T., Coppola, E., Studer, M., Firulli, A. B., Pittman, D. L. and Howard, M. J. (2008). Conditional deletion of Hand2 reveals critical functions in neurogenesis and cell type-specific gene expression for development of neural crest-derived noradrenergic sympathetic ganglion neurons. *Dev. Biol.* **319**, 179-191.

Hill, A. A. and Riley, P. R. (2004). Differential regulation of Hand1 homodimer and Hand1-E12 heterodimer activity by the cofactor FHL2. *Mol. Cell. Biol.* **24**, 9835-9847.

Hinoi, E., Bialek, P., Chen, Y. T., Rached, M. T., Groner, Y., Behringer, R. R., Ornitz, D. M. and Karsenty, G. (2006). Runx2 inhibits chondrocyte proliferation and hypertrophy through its expression in the perichondrium. *Genes Dev.* **20**, 2937-2942.

Hollenberg, S. M., Sternglanz, R., Cheng, P. F. and Weintraub, H. (1995). Identification of a new family of tissue-specific basic helix-loop-helix proteins with a two-hybrid system. *Mol. Cell. Biol.* **15**, 3813-3822.

Komori, T., Yagi, H., Nomura, S., Yamaguchi, A., Sasaki, K., Deguchi, K., Shimizu, Y., Bronson, R. T., Gao, Y. H., Inada, M. et al. (1997). Targeted disruption of Cbfa1 results in a complete lack of bone formation owing to maturational arrest of osteoblasts. *Cell* **89**, 755-764.

Martindill, D. M., Risebro, C. A., Smart, N., Franco-Viseras Mdel, M., Rosario, C. O., Swallow, C. J., Dennis, J. W. and Riley, P. R. (2007). Nucleolar release of Hand1 acts as a molecular switch to determine cell fate. *Nat. Cell Biol.* **9**, 1131-1141.

McFadden, D. G., McAnally, J., Richardson, J. A., Charité, J. and Olson, E. N. (2002). Misexpression of dHAND induces ectopic digits in the developing limb bud in the absence of direct DNA binding. *Development* **129**, 3077-3088.

McFadden, D. G., Barbosa, A. C., Richardson, J. A., Schneider, M. D., Srivastava, D. and Olson, E. N. (2005). The Hand1 and Hand2 transcription factors regulate expansion of the embryonic cardiac ventricles in a gene dosage-dependent manner. *Development* **132**, 189-201.

McLeod, M. J. (1980). Differential staining of cartilage and bone in whole mouse fetuses by alcian blue and alizarin red S. *Teratology* **22**, 299-301.

Miller, C. T., Yelon, D., Stainier, D. Y. and Kimmel, C. B. (2003). Two endothelin 1 effectors, hand2 and bapx1, pattern ventral pharyngeal cartilage and the jaw joint. *Development* **130**, 1353-1365.

Morikawa, Y., D'Autreaux, F., Gershon, M. D. and Cserjesi, P. (2007). Hand2 determines the noradrenergic phenotype in the mouse sympathetic nervous system. *Dev. Biol.* **307**, 114-126.
Mundlos, S., Otto, F., Mundlos, C., Mulliken, J. B., Aylsworth, A. S., Albright, S., Lindhout, D., Cole, W. G., Henn, W., Knoll, J. H. et al. (1997). Mutations involving the transcription factor CBFA1 cause cleidocranial dysplasia. *Cell* **89**, 773-779.
Ota, K. G., Kuraku, S. and Kuratani, S. (2007). Hagfish embryology with reference to the evolution of the neural crest. *Nature* **446**, 672-675.
Otto, F., Thornell, A. P., Crompton, T., Denzel, A., Gilmour, K. C., Rosewell, I. R., Stamp, G. W., Beddington, R. S., Mundlos, S., Olsen, B. R. et al. (1997). Cbfa1, a candidate gene for cleidocranial dysplasia syndrome, is essential for osteoblast differentiation and bone development. *Cell* **89**, 765-771.
Riley, P., Anson-Cartwright, L. and Cross, J. C. (1998). The Hand1 bHLH transcription factor is essential for placentation and cardiac morphogenesis. *Nat. Genet.* **18**, 271-275.
Risebro, C. A., Smart, N., Dupays, L., Breckenridge, R., Mohun, T. J. and Riley, P. R. (2006). Hand1 regulates cardiomyocyte proliferation versus differentiation in the developing heart. *Development* **133**, 4595-4606.
Ruest, L. B., Dager, M., Yanagisawa, H., Charité, J., Hammer, R. E., Olson, E. N., Yanagisawa, M. and Clouthier, D. E. (2003). dHAND-Cre transgenic mice reveal specific potential functions of dHAND during craniofacial development. *Dev. Biol.* **257**, 263-277.
Sauka-Spengler, T., Meulemans, D., Jones, M. and Bronner-Fraser, M. (2007). Ancient evolutionary origin of the neural crest gene regulatory network. *Dev. Cell* **13**, 405-420.
Scott, I. C., Anson-Cartwright, L., Riley, P., Reda, D. and Cross, J. C. (2000). The HAND1 basic helix-loop-helix transcription factor regulates trophoblast differentiation via multiple mechanisms. *Mol. Cell. Biol.* **20**, 530-541.
Shelton, J. M., Lee, M. H., Richardson, J. A. and Patel, S. B. (2000). Microsomal triglyceride transfer protein expression during mouse development. *J. Lipid Res.* **41**, 532-537.
Shigetani, Y., Sugahara, F., Kawakami, Y., Murakami, Y., Hirano, S. and Kuratani, S. (2002). Heterotopic shift of epithelial-mesenchymal interactions in vertebrate jaw evolution. *Science* **296**, 1316-1319.
Sierra, J., Villagra, A., Paredes, R., Cruzat, F., Gutierrez, S., Javed, A., Arriagada, G., Olate, J., Imschenetzky, M., Van Wijnen, A. J. et al. (2003). Regulation of the bone-specific osteocalcin gene by p300 requires Runx2/Cbfa1 and the vitamin D3 receptor but not p300 intrinsic histone acetyltransferase activity. *Mol. Cell. Biol.* **23**, 3339-3351.
Sosic, D., Richardson, J. A., Yu, K., Ornitz, D. M. and Olson, E. N. (2003). Twist regulates cytokine gene expression through a negative feedback loop that represses NF-kappaB activity. *Cell* **112**, 169-180.
Srivastava, D., Cserjesi, P. and Olson, E. N. (1995). A subclass of bHLH proteins required for cardiac morphogenesis. *Science* **270**, 1995-1999.
Srivastava, D., Thomas, T., Lin, Q., Kirby, M. L., Brown, D. and Olson, E. N. (1997). Regulation of cardiac mesodermal and neural crest development by the bHLH transcription factor, dHAND. *Nat. Genet.* **16**, 154-160.
Trainor, P. A. (2005). Specification of neural crest cell formation and migration in mouse embryos. *Semin. Cell Dev. Biol.* **16**, 683-693.
Vega, R. B., Matsuda, K., Oh, J., Barbosa, A. C., Yang, X., Meadows, E., McAnally, J., Pomajzl, C., Shelton, J. M., Richardson, J. A. et al. (2004). Histone deacetylase 4 controls chondrocyte hypertrophy during skeletogenesis. *Cell* **119**, 555-566.
Yamada, K., Kanda, H., Tanaka, S., Takamatsu, N., Shiba, T. and Ito, M. (2006). Sox15 enhances trophoblast giant cell differentiation induced by Hand1 in mouse placenta. *Differentiation* **74**, 212-221.
Yanagisawa, H., Hammer, R. E., Richardson, J. A., Williams, S. C., Clouthier, D. E. and Yanagisawa, M. (1998). Role of Endothelin-1/Endothelin-A receptor-mediated signaling pathway in the aortic arch patterning in mice. *J. Clin. Invest.* **102**, 22-33.
Yanagisawa, H., Clouthier, D. E., Richardson, J. A., Charite, J. and Olson, E. N. (2003). Targeted deletion of a branchial arch-specific enhancer reveals a role of dHAND in craniofacial development. *Development* **130**, 1069-1078.
Yelon, D., Ticho, B., Halpern, M. E., Ruvinsky, I., Ho, R. K., Silver, L. M. and Stainier, D. Y. (2000). The bHLH transcription factor hand2 plays parallel roles in zebrafish heart and pectoral fin development. *Development* **127**, 2573-2582.
Yoshida, C. A., Yamamoto, H., Fujita, T., Furuichi, T., Ito, K., Inoue, K., Yamana, K., Zanma, A., Takada, K., Ito, Y. et al. (2004). Runx2 and Runx3 are essential for chondrocyte maturation, and Runx2 regulates limb growth through induction of Indian hedgehog. *Genes Dev.* **18**, 952-963.